HHS Public Access

Author manuscript

J Surg Res. Author manuscript; available in PMC 2016 July 01.

Published in final edited form as:

J Surg Res. 2015 July ; 197(1): 126–138. doi:10.1016/j.jss.2015.03.023.

M1 to M2 Macrophage Polarization in HB-EGF Therapy for NEC

Jia Wei, M.D. and **Gail E. Besner, M.D.***

The Research Institute at Nationwide Children's Hospital, Center for Perinatal Research, Department of Pediatric Surgery, Nationwide Children's Hospital and the Ohio State University College of Medicine, Columbus, Ohio

Abstract

Background—Macrophages can be polarized into pro-inflammatory (M1) and anti-inflammatory (M2) subtypes. However, whether macrophage polarization plays a role in necrotizing enterocolitis (NEC) remains unknown.

Materials and methods—Macrophages were derived from the THP-1 human monocyte cell line. Apoptosis of human fetal small intestinal epithelial FHs-74 cells was determined by Annexin V/PI flow cytometry and by Western blotting to detect cleaved caspase-3. The effect of heparin-binding EGF-like growth factor (HB-EGF) on macrophage polarization was determined by flow cytometry with M1/ M2 markers and real time PCR. *In vivo*, experimental NEC was induced in mouse pups by repeated exposure to hypoxia, hypothermia and hypertonic feedings. Intestinal histologic sections were subjected to immunohistochemical staining for the detection of M1 and M2 macrophages.

Results—*In vitro*, FHs-74 cell apoptosis was increased after co-culture with macrophages and LPS. This apoptosis was increased by exposure to M1 conditioned medium (CM) and suppressed by exposure to M2 CM. HB-EGF significantly decreased LPS-induced M1 polarization and promoted M2 polarization via STAT3 activation. Addition of HB-EGF to LPS-stimulated macrophages suppressed the pro-apoptotic effects of the macrophages on FHs-74 cells. *In vivo*, we found enhanced intestinal macrophage infiltration in pups subjected to NEC, the majority of which were M1 macrophages. HB-EGF treatment of pups subjected to experimental NEC significantly reduced M1 and increased M2 polarization, and protected the intestines from NEC.

Conclusions—M1 macrophages promote NEC by increasing intestinal epithelial apoptosis. HB-EGF protects the intestines from NEC by preventing M1 and promoting M2 polarization.

Correspondence to: Gail E. Besner, M.D., Nationwide Children's Hospital, Department of Pediatric Surgery, ED383, 700 Children's Drive, Columbus, OH 43205, (614) 722-3914 (Phone), (614) 722-3990 (FAX), gail.besner@nationwidechildrens.org.

Disclosure

The authors reported no proprietary or commercial interest in any product mentioned or concept discussed in the article.

Authors' contributions: J.W and G.E.B contributed to the project conception and design. J.W. collected and analyzed the data, and prepared the manuscript. G.E.B analyzed and interpreted the data, and critically revised and approved the final manuscript.

Keywords

Heparin-Binding EGF-Like Growth Factor (HB-EGF); macrophage polarization; necrotizing enterocolitis

1. Introduction

Necrotizing enterocolitis (NEC) is the most common cause of gastrointestinal mortality in newborns, typically affecting babies born prematurely with low birth weight. NEC affects ~7% of infants with a birth weight between 500 and 1,500g. The overall mortality rate associated with NEC is between 20 and 30% [1]. Despite over six decades of research, the pathogenesis of the disease remains unclear.

Recent studies indicate that macrophages play an essential role in the development of NEC. Neonatal NEC has been shown to be associated with macrophage-rich infiltration in human NEC samples and experimental mouse NEC samples [2]. In addition, IL-18 knockout mice have been shown to have decreased intestinal macrophages, associated with less severe NEC injury [3]. Furthermore, the premature innate immune system is associated with a hyper-inflammatory intestinal macrophage phenotype that causes increased NEC injury [4].

Macrophages play a critical role in the development, progression and resolution of inflammation. Two subtypes of polarized macrophages are classical macrophages (M1) and alternative macrophages (M2). Activated M1 macrophages are pro-inflammatory macrophages induced by IFN-γ and TLR ligands. M1 macrophages produce inflammatory cytokines such as IL-6, nitric oxide (NO) and tumor necrosis factor-α (TNF-α), and contribute to inflammation. In contrast, M2 macrophages are anti-inflammatory and promote tissue remodeling. Previous studies have shown that macrophages are plastic cells, and that M1 and M2 macrophages can switch their functional profiles in response to micro-environmental change [5, 6]. Moreover, M2 macrophage polarization has been reported to contribute to the ability of mesenchymal stem cells to ameliorate acute kidney injury [7] and to protect the lungs from endotoxemia and acute lung injury [8]. Thus, therapeutic modulation of immune responses from M1 macrophages towards M2 macrophages may be critical to the development of novel therapeutic strategies for NEC.

Heparin-binding epidermal growth factor-like growth factor (HB-EGF) was initially isolated from cultured human macrophages [9] and was later found to be a member of the epidermal growth factor (EGF) family [10]. We have previously demonstrated that administration of HB-EGF protects the intestines from histologic injury in models of experimental NEC [11], intestinal ischemia-reperfusion (I/R) injury [12, 13], hemorrhagic shock and resuscitation [14], and radiation exposure [15], and that intraluminal administration of HB-EGF significantly reduces intestinal I/R-induced production of pro-inflammatory cytokines including TNF-α, IL-6 and IL-1β [16]. Although the role of HB-EGF in promoting cell proliferation and migration is well established, its function in regulating macrophage polarization is poorly understood.

The goal of the current study was to investigate the role of macrophage polarization in experimental NEC, and to determine the ability of HB-EGF to regulate the intestinal inflammatory immune response and macrophage polarization *in vitro* and in a murine NEC model *in vivo*.

2. Materials and Methods

2.1. FHs-74 Int cell culture

The FHs-74 Int human fetal small intestinal cell line (derived from a female) (ATCC, Manassas, VA) was cultured in DMEM (Gibco, Grand Island, NY, USA) containing 10% fetal bovine serum (FBS; Gibco, Grand Island, NY, USA), 30 ng/ml EGF (Gibco, Grand Island, NY, USA) and 10 μg/ml insulin (Gibco, Grand Island, NY, USA).

2.2. Preparation and stimulation of macrophage conditioned medium

The THP-1 human monocytic cell line (ATCC, Manassas, VA) was cultured in RPMI-1640 Medium (ATCC, Manassas, VA) supplemented with 10% (v/v) FBS (Gibco, Grand Island, NY) and 0.05nM 2-mercaptoethanol (Gibco, Grand Island, NY). THP-1 cells were treated with 10 ng/ml Phorbol 12-myristate 13-acetate (PMA, Sigma-Aldrich, St. Louis, MO) for 48h to generate macrophages. Following differentiation, macrophages were washed and then treated with the following additives to their culture medium: 1) no additional additive to maintain M0 macrophages; 2) 100 ng/ml LPS (Sigma-Aldrich, St. Louis, MO) and 20 ng/ml IFN-γ (eBioscince, San Diego, CA) to produce M1 macrophages; 3) 20 ng/ml IL-4 (Life Technologies, Grand Island, NY) and 20 ng/ml IL-13 (Shenanboah Biotechnology, Warwick, PA) to produce M2 macrophages; 4) 100 ng/ml HB-EGF; 5) 100 ng/ml LPS; or 6) 100 ng/ml HB-EGF + 100 ng/ml LPS. After incubation for 24h, medium was removed and all cells were washed 3 times with PBS to remove residual LPS and other additives, and then the cells were cultured in fresh DMEM supplemented with 10% FBS for 8h. Supernatant conditioned medium (CM) was collected from each cell group and labeled as follows: 1) M0 CM, 2) M1 CM, 3) M2 CM, 4) HB-EGF CM, 5) LPS CM, and 6) HB-EGF+LPS CM.

2.3. Quantitative real time PCR (qRT-PCR)

Total RNA from macrophages derived from THP-1 cells was extracted using RNA STAT-60 (TEL-TEST, Friendswoods, TX) according to the manufacturer's protocol. Aliquots of 1μg of total RNA were reverse transcribed using SuperScript II Reverse Transcriptase (Invitrogen, Carlsbad, CA) and oligo-dT (18)-primers (Invitrogen, Carlsbad, CA). The real time PCR reaction was performed using SYBR Green Master Mix kit in ABI Prism 7000 Sequence Detection System (Applied Biosystems, Forster City, CA) according to the manufacturer's instructions. Glyceraldehyde-3-phosphate dehydrogenase (GAPDH) was amplified as an internal standard. The primers used are shown in Table I. The expression levels of the mRNAs were reported as fold changes *vs.* control.

2.4. Flow cytometry for macrophage subtype analysis

M1 macrophages were recognized by immunophenotype using monoclonal antibodies specific for F4/80-APC and CD86-FITC (BD Biosciences, San Jose, CA), and M2 macrophages were identified with antibodies specific for anti-F4/80-APC and anti–CD206-

PE-Cy5 antibodies (BD Biosciences, San Jose, CA). For immunophenotypic analysis, macrophages were gently detached by a cell scraper, pipetted into single cells, and suspended at 2×10^6/ml. Cell suspensions were incubated for 15 min with 10% goat serum, following by incubation with the antibody mixtures for 30 min on ice. Cells were then washed with PBS containing 2% FBS twice. Data were immediately acquired using BD LSR II (BD Biosciences, San Jose, CA) using Flowjo software (Tree Star, San Carlos, CA). Gating strategies are shown in the figure legends.

2.5. Flow-cytometry for apoptosis detection

Apoptosis of FHs-74 cells was measured using an annexin V-FITC apoptosis detection kit (BD Pharmingen, San Diego, CA) according to the manufacturer's protocol. Briefly, FHs-74 cells were harvested, washed in PBS, and stained with annexin V-FITC and propidium iodide (PI) in binding buffer at RT for 15 min. Samples were detected with BD LSR II (BD Biosciences, San Jose, CA) and 20,000 cells were analyzed for each sample. Data were analyzed using Flow Jo software (Tree Star, San Carlos, CA).

2.6. Western blot analysis

FHs-74 cells were lysed in buffer containing 50 mM Tris-HCl, 150 mM NaCl, 1% Triton X-100,1 mM EDTA, 1 mM EGTA, 50 mM NaF, 10 mM β-glycerophosphate, 5 mM sodium pyrophosphate, and 2 μg/ml protease inhibitors (Roche, San Francisco, CA). Clarified cytosolic extracts were subjected to SDS-PAGE followed by Western blot analysis using rabbit anti-human cleaved caspase-3 mAb (1:1000, Cell Signaling, Beverly, MA). Protein bands were detected with ECL detection reagents (Amersham Biosciences, Piscataway, NJ) using Hyperfilm (Amersham Biosciences, Piscataway, NJ) for exposure. To standardize protein loading, membranes were stripped and probed with anti-β-actin antibodies (1:3000, Sigma-Aldrich, St. Louis, MO). β-actin was used to normalize densities of cleaved caspase bands. Bands were quantified by densitometry using Image J Software.

2.7. Knock-down of expression of signal transducers and activators of transcription 3 (STAT3)

Differentiation of THP-1 cells to macrophages was performed 48h prior to transfection. Macrophages were detached using Accutase I (Thermo Electron, Louisville, CO) and transfected using the Amaxa Basic Nucleofector kit (Lonza, Allendale, NJ) and the Amaxa Nucleofactor II apparatus (Lonza, Allendale, NJ) with either human STAT3 siRNA (200nM) or human scrambled siRNA (200nM) (all from Ambion, Carlsbad, CA). Transfected cells were then seeded into 6-well plates (2×10^6 cells/well) for an additional 24h in RPMI-1640 Medium (ATCC, Manassas, VA) supplemented with 10% (v/v) FBS (Gibco, Grand Island, NY), 0.05nM 2-mercaptoethanol (Gibco, Grand Island, NY) and 10 ng/ml Phorbol 12-myristate 13-acetate (PMA, Sigma-Aldrich, St. Louis, MO) for 24h. Macrophages were then washed and treated with the following additives to the culture medium: 1) no additional additive; 2) HB-EGF (100 ng/ml); or 3) HB-EGF (100 ng/ml) + LPS 100 (ng/ml).

2.8. Murine Model of NEC

The following experimental protocols followed the guidelines for the ethical treatment of experimental animals as approved by the Institutional Animal Care and Use Committee of the Research Institute at Nationwide Children's Hospital (protocol #02205 AR). C57/BL6 mice were randomized into the following groups: (1) breast fed (Vehicle) (n=17); (2) NEC (n=48); (3) NEC + gastric gavage of HB-EGF (800 μg/kg/dose) with each feed (n=27). NEC was induced using a modification of the model initially described by Barlow *et al.* [17] and modified for mice by Jilling *et al*. [18]. Mouse pups (male and female) were collected after vaginal delivery and prior to breast feeding. They were recovered, dried and placed in an incubator at 35°C. Pups were fed Similac 60/40 (Ross Pediatrics, Columbus, OH) formula fortified with Esbilac powder (Pet-Ag, New Hampshire, IL) which provided 836.8 kJ/kg per day as we have described [19]. Pups were exposed to hypoxia (95% nitrogen for 1 min) followed by hypothermia (4° C for 10 min) every 12 hours. Pups were sacrificed upon the development of clinical signs of NEC including abdominal distention, bloody stools or respiratory distress. Any surviving pups were sacrificed 96 h after birth. Pups were treated with enteral HB-EGF (800 μg/kg/dose) added to each feed by adding HB-EGF into the formula. Intestines were harvested immediately upon sacrifice.

2.9. Immnuofluorescence staining

Intestines were fixed in 4% paraformaldehyde, embedded in paraffin, and 4 μm thick tissue sections obtained. Tissue sections were subjected to immunohistochemistry using the following specific primary antibodies: mouse anti-CD68 (1:100, Novus biologicals, Littleton, CO) to detect total macrophages, rabbit anti-CD86 (1:100, Abcam, Cambridge, MA) to detect M1 macrophages, and rabbit anti-CD206 (0.1μg/ml, Abcam, Cambridge, MA) to detect M2 macrophages. After washing in PBS, tissue sections were incubated with fluorophore-conjugated goat anti-mouse IgG (1:400, Alexa 647, Molecular Probes, Eugene, OR) or anti-rabbit IgG (1:400, Alexa 488, Molecular Probes, Eugene, OR) as appropriate. Sections were counterstained with 4′6-diamidino-2-phenylindole (DAPI). Fluorescence images were obtained by confocal microscopy (LSM 710, Carl Zeiss, Thornwood, NY) and images analyzed using Image J software (Media cybernetics, Silver Springs, MD).

2.10. Statistical analyses

All values are presented as mean ± SD. After confirming that all variables were normally distributed using the Kolmogorov-Smirnov test, statistical differences were evaluated by ANOVA followed by Bonferroni's multiple comparison test. Differences in the incidence of NEC between two groups were evaluated using the Fisher's exact test. P values of <0.05 were considered statistically significant.

3. Results

3.1. Macrophages enhance LPS-induced FHs-74 cell apoptosis *in vitro*

To evaluate a potential role for macrophages in LPS-induced IEC apoptosis, we examined apoptosis of FHs-74 human fetal intestinal epithelial cells exposed to LPS alone, macrophage co-culture alone, or a combination of LPS + macrophage co-culture as determined by flow-cytometry and Western blot analysis. FITC-annexin V/PI flow

cytometry showed that the percentage of apoptotic FHs-74 cells was increased after LPS exposure × 24h compared to control cells (25.0% ± 2.0% *vs.* 9.1% ± 0.8%, $p<0.01$) (Figure 1A,B). Apoptosis of FHs-74 cells was further increased after co-culture of LPS-treated cells with macrophages (34.4% ± 3.8% vs. 25.0% ± 2.0%, $P= 0.04$). Macrophage co-culture alone did not induce apoptosis of FHs-74 cells (11.7% ± 2.6% *vs*. 9.1% ± 0.8%, $p=0.116$). Further confirmation of these results was obtained by cleaved caspase-3 Western blotting. Cleaved caspase-3 expression in FHs-74 cells was increased after exposure to LPS, and was further increased when LPS-treated FHs-74 cells were co-cultured with macrophages (Figure 1C). These results indicate that macrophages enhance LPS-induced FHs-74 cell apoptosis.

3.2. M1 macrophages increase LPS-induced FHs-74 cell apoptosis and M2 macrophages decrease LPS-induced FHs-74 cell apoptosis induced *in vitro*

LPS is well known to induce macrophages towards M1 polarization. To determine whether polarization of macrophages affects LPS-induced IEC apoptosis, we examined the effects of CM from activated-macrophage cultures on FHs-74 cells. Flow cytometry using FITC-annexin V/PI staining demonstrated that M1 macrophage conditioned medium (M1 CM) significantly increased the percent of apoptotic FHs-74 cells (20.9% ± 1.5% *vs.* 11.45% ± 2.1%, $p<0.01$) and further increased the percent of apoptotic FHs-74 cells after LPS exposure compared to M0 (untreated) macrophage CM (M0 CM) (36.3% ± 2.5% *vs.* 28.3% ± 3.2%, $p<0.01$) (Figure 2A,B). In contrast, M2 macrophage CM (M2 CM) significantly decreased apoptosis of FHs-74 cells after LPS exposure compared to apoptosis of FHs-74 cells exposed to M0 CM after LPS exposure (23.5% ± 2.2% *vs.* 28.3% ± 3.2%, $p<0.05$). As determined by Western blotting, increased cleaved caspase-3 expression was found in FHs-74 cells exposed to M1 CM, which was further increased after LPS exposure (Figure 2C). Conversely, M2 CM suppressed the effect of LPS on cleaved caspase-3 expression. Thus, the CM from M1 macrophages enhances IEC apoptosis and the CM M2 protects IEC from apoptosis.

3.3. HB-EGF promotes M1 to M2 macrophage polarization *in vitro*

Having demonstrated that macrophage polarization affects IEC apoptosis, we next investigated the effects of HB-EGF on macrophage polarization as determined by flow cytometry and real time RT-PCR. M1 macrophages and M2 macrophages were identified as viable CD68+CD86+ cells and CD68+CD206+ cells respectively on flow cytometry. Flow cytometric analysis of macrophages derived from THP-1 cells showed the identification of distinct subsets. M1 macrophages predominated in the total macrophages exposed to LPS alone (83.1% ± 4.8%) (Figure 3A,C). The proportion of M1 macrophages significantly decreased with increasing doses of HB-EGF during LPS exposure. Conversely, LPS markedly decreased the proportion of M2 macrophages, whereas the proportion of M2 macrophages exposed to LPS was significantly increased in a dose-dependent fashion with HB-EGF addition (Figure 3B,C).

For qRT-PCR, CD86 and inducible nitric oxide synthase (iNOS) served as M1 macrophage markers, while CD206, peroxisome proliferation activated receptor-gamma (PPAR-γ) and Arginase-1 (Arg-1) served as M2 macrophage markers. mRNA expression of the M1

macrophage markers CD86 and iNOS were significantly increased after exposure of macrophages to LPS, and were significantly decreased after addition of HB-EGF during LPS exposure (Figure 4A). In contrast, mRNA expression of the M2 macrophage markers CD206, PPAR-γ, and Arg-1 were significantly decreased after exposure of macrophages to LPS, and HB-EGF significantly increased their mRNA expression during LPS exposure (Figure 4B). Taken together, these results demonstrate that HB-EGF promotes M1 to M2 macrophage polarization.

3.4. HB-EGF treatment of macrophages protects FHs-74 cells from LPS-induced apoptosis *in vitro*

To determine whether HB-EGF protects FHs-74 cells from LPS-induced apoptosis induced by a direct effect on macrophages, we collected CM from supernatants of HB-EGF-treated macrophages (HB-EGF CM), LPS-treated macrophages (LPS CM), a combination of HB-EGF- and LPS-treated macrophages (HB-EGF+LPS CM), and non-treated control macrophages. Flow-cytometry for FITC Annexin V/PI showed that LPS CM significantly increased the percent of apoptotic FHs-74 cells compared to control (19.9% ± 2.2% *vs.* 10.9% ± 0.8%, $p<0.01$) (Figure 5A,B). HB-EGF + LPS CM decreased the percent of apoptotic FHs-74 cells compared to LPS CM (15.0% ± 1.5% *vs.* 19.9% ± 2.2%, $p=0.012$). After LPS exposure, addition of LPS CM further increased apoptosis of FHs-74 cells compared to LPS exposure alone (37.2% ± 5.2% *vs.* 27.7% ± 2.5%, $p<0.01$). Addition of HB-EGF CM significantly decreased apoptosis of FHs-74 cells compared to LPS exposure alone (20.7% ± 2.2% *vs.* 27.7% ± 2.5%, $p<0.05$). Moreover, after LPS exposure, HB-EGF + LPS CM significantly decreased the the percentage of apoptotic FHs-74 cells compared to LPS CM (29.36% ± 2.2% *vs.* 37.2% ± 5.2%, $p<0.05$). Western blot analysis confirmed the flow cytometry results (Figure 5C).

3.5. HB-EGF promotes macrophage polarization via STAT3

HB-EGF is known to activate STAT3 in glioma cells [20], and STAT3 is known to promote macrophage M2 polarization [21]. Based on these observations, we next tested whether the STAT3 pathway is involved in HB-EGF-induced macrophage M2 polarization. STAT3 siRNA transfection of macrophages significantly reduced STAT3 mRNA expression compared to scrambled siRNA transfection (Figure 6A). Flow cytometry results showed that HB-EGF-induced macrophage M2 polarization in the presence or absence of LPS was significantly blocked by siRNA silencing of STAT3 (Figure 6B,C). Quantitative real time PCR analysis of M2 markers CD206, Arg-1 and PPARγ, confirmed the role of STAT3 in HB-EGF-induced macrophage M2 polarization since STAT3 silencing significantly suppressed HB-EGF-induced mRNA expression of these M2 markers in the presence or absence of LPS (Figure 6D).

3.6. HB-EGF promotes a phenotypic switch from M1 macrophages to M2 macrophages during experimental NEC *in vivo*

We first determined whether macrophage infiltration in the intestines occurs in experimental NEC, and then evaluated whether HB-EGF affects macrophage polarization *in vivo*. Immunohistochemistry using anti-CD68, anti-CD86 and anti-CD206 antibodies was used to

detect total macrophages, M1 macrophages and M2 macrophages, respectively (Figure 7). Increased total ($CD68^+$) macrophage infiltration was observed in the intestines of pups subjected to NEC compared to breast fed pups (22.9 ± 5.8 cells/ visual field *vs.* 11.9 ± 2.1 cells / visual field, $p<0.01$) (Figure 7C). The majority of infiltrated macrophages in NEC intestine expressed M1 macrophage markers (M1 *vs.* M2: 63.5% ± 12.0% *vs.* 7.7% ± 5.4%, $P<0.01$) (Figure 2D). Compared to untreated pups subjected to NEC, pups that were treated with HB-EGF had significantly reduced numbers of M1 macrophages (8 ± 1.47 cells/ visual field *vs.* 13.63 ± 3.61 cells/ visual field, $p<0.05$), as well as the percent of M1 macrophages/ total macrophages (45.3% ± 3.9% *vs.* 63.5% ± 12.0%, $p<0.05$). In contrast, HB-EGF treatment markedly increased M2 macrophages (7.0 ± 1.5 cells/ visual field *vs.* 1.8 ± 1.3 cells/ visual field, $p<0.01$) as well as the percent of M2 macrophages/total macrophages (39.7% ± 9.7% *vs.* 7.7% ± 5.4%, $p<0.01$) compared to non-treated pups exposed to NEC. These results suggest that HB-EGF promotes the polarization of macrophages from an M1 to an M2 phenotype during experimental NEC.

3.7. HB-EGF protects the intestines from experimental NEC injury *in vivo*

Pups exposed to experimental NEC had a significantly increased incidence of histological injury compared to breast fed pups (68.8% *vs.* 0%, $p<0.01$) (Figure 8A). Pups exposed to NEC that received enteral HB-EGF had a significantly decreased incidence of NEC compared to non-treated pups subjected to NEC (38.4% *vs.* 68.8%, p=0.012) (Figure 8B). These results confirm that HB-EGF protects the intestines from injury during experimental NEC.

4. Discussion

The immune system plays an important role during NEC. Previous work has shown that an exaggerated inflammatory response in the immune system of premature hosts causes severe intestinal inflammation such as that seen in NEC [4]. Macrophages are extremely important host cells in the innate immune system. Epithelial cells in the fetal intestine produce chemerin to recruit macrophages [22] whose presence in the fetal intestine precedes the appearance of lymphocytes and neutrophils. Investigations of the pathogenic role of macrophages in NEC have focused on their infiltration and their ability to produce inflammatory cytokines [2, 4, 23]. The increased levels of IFN-γ and TNF-α in both the diseased gut and the serum of patients with NEC [24], together with large amounts of LPS, can provide ample stimulation to macrophages in both the peripheral blood and in the mucosa and submucosa of the intestines of these patients.

It is well known that macrophages have a plastic ability to switch between two functional phenotypes, designated as pro-inflammatory M1 macrophages and anti-inflammatory M2 macrophages, in response to environment changes. Classically activated M1 macrophages act as initiators of inflammation, with release of pro-inflammatory cytokines including IL-1β, iNOS and TNF-α. In comparison, M2 macrophages can up-regulate the expression of IL-10, TGF-β, and other molecules that are involved in cell proliferation, wound healing, tissue remodeling and immnuoregulation [25, 26], and are considered beneficial in that they promote resolution of M1 macrophage-mediated inflammation. Thus, macrophages show a functional plasticity during the initiation and resolution of inflammation. A phenotypic

switch to M2 polarization has been suggested as a novel approach to reducing inflammation in a model of inflammatory muscle pain [27] and in a model of experimental asthma [28].

In the current study, we investigated the effects of HB-EGF on macrophage polarization both *in vitro*, and *in vivo* using a model of experimental NEC. *In vitro*, we showed that M1 macrophages enhance LPS-induced apoptosis of human intestinal epithelial cells whereas M2 macrophages suppress this effect. We showed that macrophages contribute to LPS-induced apoptosis of human fetal epithelial cells. M1 macrophages further enhance this apoptosis while M2 macrophages suppress it. We showed that HB-EGF promotes the polarization of M1 macrophages toward M2 macrophages by activation of STAT3 *in vitro*, and protects human fetal intestinal epithelial cells from apoptosis. *In vivo*, we showed that M1 macrophages are significantly increased in NEC-afflicted intestine, and that HB-EGF reduces the number of M1 macrophages and increases the number of M2 macrophages during NEC, and protects the intestines from NEC. We showed that the total number of macrophages is significantly increased in the intestines of pups exposed to NEC compared to breast fed pups. Although we and others have described increased macrophage infiltration in the intestines of animals with NEC [2, 29], the current results extend these prior observations by demonstrating that M1 macrophages represent the majority of infiltrated macrophages during NEC.

It is known that M1 macrophages promote apoptosis by various mechanisms, including the secretion of pro-apoptotic cytokines such as TNF-α and others [30]. We believe that in our studies, M1 macrophages first become activated and then mediate IEC apoptosis via paracrine mechanisms. However, a large number of cytokines are likely to be released, and determining which ones contribute to IEC apoptosis, although beyond the scope of the current manuscript, will be examined in the future. The contributing roles of intestinal epithelial cell Toll-like receptor expression warrants examination in the future as well.

We have previously shown that HB-EGF protects the intestines from NEC [11] and that administration of HB-EGF significantly reduces intestinal I/R-induced pro-inflammatory cytokine expression *in vivo* [16]. We now show that HB-EGF promotes M2 macrophage polarization in a STAT3-dependent fashion. HB-EGF interacts with EGFR [10], which activates downstream signal transducers and activators of transcription 3 (STAT3) in the nucleus [31]. Others have reported that human macrophages can be induced to M2 polarization via SATA3 activation [21] and that suppression of STAT3 activation inhibits macrophage polarization to the M2 phenotype [32]. Taking together, EGFR/STAT3 may be the signal pathway through which HB-EGF promotes M2 polarization.

5. Conclusions

Our current results suggest that M1 macrophages may play an important role in the pathogenesis of NEC. HB-EGF promotes the polarization M1 macrophages to M2 macrophages via STAT3, reduces LPS-induced apoptosis of intestine epithelial cells, and protects the intestines from NEC injury. These findings provided novel insights into the pathogenesis of NEC, and into the effect of HB-EGF in the treatment of NEC. These results

suggest that new therapeutic approaches for NEC, based on the regulation of macrophage polarization, may be beneficial.

Acknowledgments

This research was supported by NIH R01 DK74611 and GM61193 (GEB). The funding sources had no direct involvement in study design, collection or interpretation of data, writing of the report, or decision to submit the article for publication. We thank the Flow Cytometry Core at The Research Institute at Nationwide Children's Hospital for technical support and thank Dr. Yu Zhou for helpful discussions.

References

1. Fitzgibbons SC, Ching Y, Yu D, et al. Mortality of necrotizing enterocolitis expressed by birth weight categories. J Pediatr Surg. 2009; 44:1072–5. discussion 5–6. [PubMed: 19524719]
2. MohanKumar K, Kaza N, Jagadeeswaran R, et al. Gut mucosal injury in neonates is marked by macrophage infiltration in contrast to pleomorphic infiltrates in adult: evidence from an animal model. Am J Physiol Gastrointest Liver Physiol. 2012; 303:G93–102. [PubMed: 22538401]
3. Halpern MD, Khailova L, Molla-Hosseini D, et al. Decreased development of necrotizing enterocolitis in IL-18-deficient mice. Am J Physiol Gastrointest Liver Physiol. 2008; 294:G20–6. [PubMed: 17947451]
4. Maheshwari A, Kelly DR, Nicola T, et al. TGF-beta2 suppresses macrophage cytokine production and mucosal inflammatory responses in the developing intestine. Gastroenterology. 2011; 140:242–53. [PubMed: 20875417]
5. Hussell T, Bell TJ. Alveolar macrophages: plasticity in a tissue-specific context. Nat Rev Immunol. 2014; 14:81–93. [PubMed: 24445666]
6. Murray PJ, Wynn TA. Protective and pathogenic functions of macrophage subsets. Nat Rev Immunol. 2011; 11:723–37. [PubMed: 21997792]
7. Geng Y, Zhang L, Fu B, et al. Mesenchymal stem cells ameliorate rhabdomyolysis-induced acute kidney injury via the activation of M2 macrophages. Stem Cell Res Ther. 2014; 5:80. [PubMed: 24961539]
8. Grailer JJ, Haggadone MD, Sarma JV, et al. Induction of M2 Regulatory Macrophages through the beta-Adrenergic Receptor with Protection during Endotoxemia and Acute Lung Injury. J Innate Immun. 2014
9. Besner G, Higashiyama S, Klagsbrun M. Isolation and characterization of a macrophage-derived heparin-binding growth factor. Cell Regul. 1990; 1:811–9. [PubMed: 2088527]
10. Higashiyama S, Abraham JA, Miller J, et al. A heparin-binding growth factor secreted by macrophage-like cells that is related to EGF. Science. 1991; 251:936–9. [PubMed: 1840698]
11. Feng J, El-Assal ON, Besner GE. Heparin-binding epidermal growth factor-like growth factor decreases the incidence of necrotizing enterocolitis in neonatal rats. J Pediatr Surg. 2006; 41:144–9. discussion-9. [PubMed: 16410124]
12. Pillai SB, Hinman CE, Luquette MH, et al. Heparin-binding epidermal growth factor-like growth factor protects rat intestine from ischemia/reperfusion injury. J Surg Res. 1999; 87:225–31. [PubMed: 10600353]
13. El-Assal ON, Besner GE. Heparin-binding epidermal growth factor-like growth factor and intestinal ischemia-reperfusion injury. Semin Pediatr Surg. 2004; 13:2–10. [PubMed: 14765365]
14. Zhang HY, James I, Chen CL, et al. Heparin-binding epidermal growth factor-like growth factor (HB-EGF) preserves gut barrier function by blocking neutrophil-endothelial cell adhesion after hemorrhagic shock and resuscitation in mice. Surgery. 2012; 151:594–605. [PubMed: 22153812]
15. Matthews MA, Watkins D, Darbyshire A, et al. Heparin-binding EGF-like growth factor (HB-EGF) protects the intestines from radiation therapy-induced intestinal injury. J Pediatr Surg. 2013; 48:1316–22. [PubMed: 23845625]
16. Rocourt DV, Mehta VB, Besner GE. Heparin-binding EGF-like growth factor decreases inflammatory cytokine expression after intestinal ischemia/reperfusion injury. J Surg Res. 2007; 139:269–73. [PubMed: 17291530]

17. Barlow B, Santulli TV, Heird WC, et al. An experimental study of acute neonatal enterocolitis--the importance of breast milk. J Pediatr Surg. 1974; 9:587–95. [PubMed: 4138917]
18. Jilling T, Simon D, Lu J, et al. The roles of bacteria and TLR4 in rat and murine models of necrotizing enterocolitis. J Immunol. 2006; 177:3273–82. [PubMed: 16920968]
19. Radulescu A, Zhang HY, Yu X, et al. Heparin-binding epidermal growth factor-like growth factor overexpression in transgenic mice increases resistance to necrotizing enterocolitis. J Pediatr Surg. 2010; 45:1933–9. [PubMed: 20920709]
20. Zhou M, Wang H, Zhou K, et al. A novel EGFR isoform confers increased invasiveness to cancer cells. Cancer Res. 2013; 73:7056–67. [PubMed: 24240702]
21. Shiraishi D, Fujiwara Y, Komohara Y, et al. Glucagon-like peptide-1 (GLP-1) induces M2 polarization of human macrophages via STAT3 activation. Biochem Biophys Res Commun. 2012; 425:304–8. [PubMed: 22842565]
22. Maheshwari A, Kurundkar AR, Shaik SS, et al. Epithelial cells in fetal intestine produce chemerin to recruit macrophages. Am J Physiol Gastrointest Liver Physiol. 2009; 297:G1–G10. [PubMed: 19443732]
23. Tan X, Hsueh W, Gonzalez-Crussi F. Cellular localization of tumor necrosis factor (TNF)-alpha transcripts in normal bowel and in necrotizing enterocolitis. TNF gene expression by Paneth cells, intestinal eosinophils, and macrophages. Am J Pathol. 1993; 142:1858–65. [PubMed: 8506954]
24. Ford HR, Sorrells DL, Knisely AS. Inflammatory cytokines, nitric oxide, and necrotizing enterocolitis. Semin Pediatr Surg. 1996; 5:155–9. [PubMed: 8858761]
25. Biswas SK, Chittezhath M, Shalova IN, et al. Macrophage polarization and plasticity in health and disease. Immunol Res. 2012; 53:11–24. [PubMed: 22418728]
26. Mantovani A, Biswas SK, Galdiero MR, et al. Macrophage plasticity and polarization in tissue repair and remodelling. J Pathol. 2013; 229:176–85. [PubMed: 23096265]
27. da Silva MD, Bobinski F, Sato KL, et al. IL-10 Cytokine Released from M2 Macrophages Is Crucial for Analgesic and Anti-inflammatory Effects of Acupuncture in a Model of Inflammatory Muscle Pain. Mol Neurobiol. 2014
28. Song X, Xie S, Lu K, et al. Mesenchymal Stem Cells Alleviate Experimental Asthma by Inducing Polarization of Alveolar Macrophages. Inflammation. 2014
29. Xia G, Martin AE, Besner GE. Heparin-binding EGF-like growth factor downregulates expression of adhesion molecules and infiltration of inflammatory cells after intestinal ischemia/reperfusion injury. J Pediatr Surg. 2003; 38:434–9. [PubMed: 12632363]
30. Jaiswal MK, Agrawal V, Mallers T, et al. Regulation of apoptosis and innate immune stimuli in inflammation-induced preterm labor. J Immunol. 2013; 191:5702–13. [PubMed: 24163412]
31. Lo HW, Hsu SC, Ali-Seyed M, et al. Nuclear interaction of EGFR and STAT3 in the activation of the iNOS/NO pathway. Cancer Cell. 2005; 7:575–89. [PubMed: 15950906]
32. Fujiwara Y, Takeya M, Komohara Y. A novel strategy for inducing the antitumor effects of triterpenoid compounds: blocking the protumoral functions of tumor-associated macrophages via STAT3 inhibition. Biomed Res Int. 2014; 2014:348539. [PubMed: 24738052]

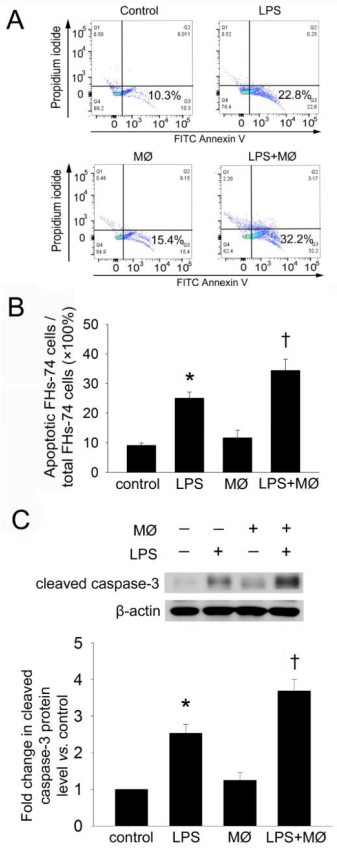

Figure 1. Effect of macrophage co-culture on LPS-induced FHs-74 cell apoptosis

FHs-74 cells were either untreated (Control); exposed to LPS (1 μg/ml); co-cultured with macrophages in a transwell system; or exposed to LPS (1 μg/ml) and co-cultured with macrophages. After 24h, the FHs-74 cells were harvested and analyzed by Annexin V/PI flow cytometry. Gating was performed on FITC-Annexin V^+ cells. (A) Representative FACS plot. (B) Quantification of results from A. Data represent the mean ± SD of four independent experiments. *$p<0.01$ *vs.* cont**rol;** † $p<0.05$ vs. LPS. (C) Western blot analysis of cleaved caspase-3 expression in FHs-74 cells. The expression level of cleaved caspase-3 was normalized against the level of untreated FHs-74 cells, which was arbitrarily set as 1. The data shown are the mean ± SD of three independent experiments. * $p<0.01$ *vs.* **control;** † $p<0.05$ vs. LPS.

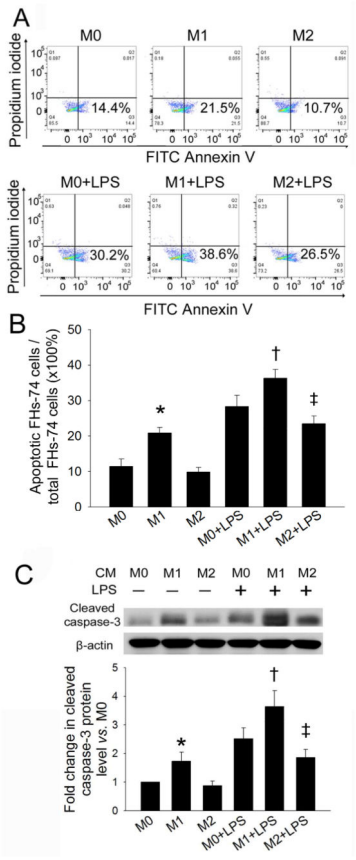

Figure 2. Effect of M1 and M2 CM on LPS-induced FHs-74 cell apoptosis

Macrophages derived from THP-1 cells were either unstimulated (M0) or were polarized into M1 or M2 cells for 24h and supernatant CM harvested. FHs-74 cells were exposed to CM or CM + LPS (1μg/ml) for 24h and then harvested for Annexin V/PI flow cytometry. Gating was performed on FITC-Annexin V^+ cells. (A) Representative FACS plots. (B) Quantification of results from A. Data represent the mean ± SD of four independent experiments. * $p<0.01$ *vs.* M0**; †** $p<0.05$ vs. **M0+LPS; ‡** $p<0.05$ *vs.* M0+LPS. (C) Western blot analysis of cleaved caspase-3 expression in FHs-74 cells. The expression level of cleaved caspase-3 was normalized against the level of FHs-74 cells incubated with M0 CM, which was arbitrarily set as 1. The data shown are the mean ± SD of three independent experiments. $p<0.01$ *vs.* **M0; †** $p<$**0.05 vs. M0+LPS; ‡** $p<0.05$ *vs.* M0+LPS.

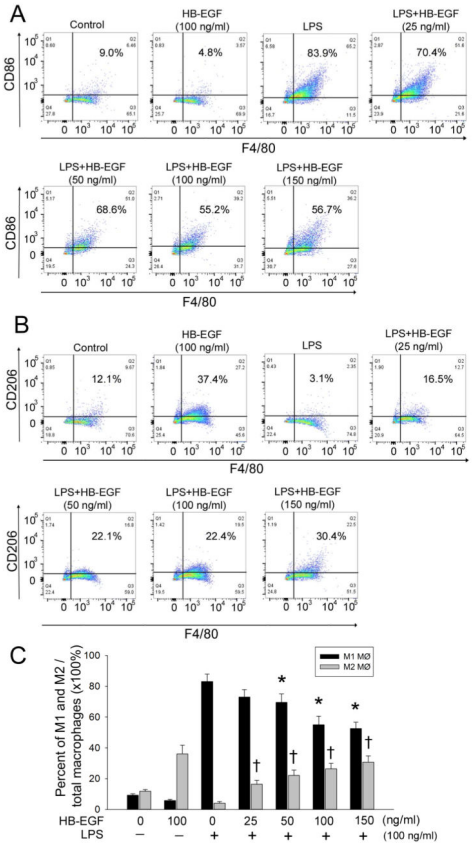

Figure 3. Effect of HB-EGF on macrophage polarization as determined by flow cytometry

Macrophages derived from THP-1 cells were exposed to the indicated conditions for 24h. (A) M1 macrophages were labeled with FITC-conjugated anti-human CD86 and APC-conjugated anti-human F4/80 antibodies and the percent of M1 macrophages/total macrophages determined by flow cytometry. Representative FACS plots are shown. Gating was performed on F4/80 $^{+}$/CD86^{+} cells. (B) M2 macrophages were labeled with PE-Cy5-conjugated anti-human CD206 and APC-conjugated anti-human F4/80 antibodies and then analyzed the percentage of M2 macrophages/total macrophages by flow cytometry. Representative FACS plots are shown. Gating was performed on F4/80 $^{+}$/CD206^{+} cells. (C) Quantification of data from A and B. Data represent the mean ± SD of four independent experiments. * $p<0.05$ *vs.* **LPS alone;** † $p<0.05$ *vs.* LPS alone.

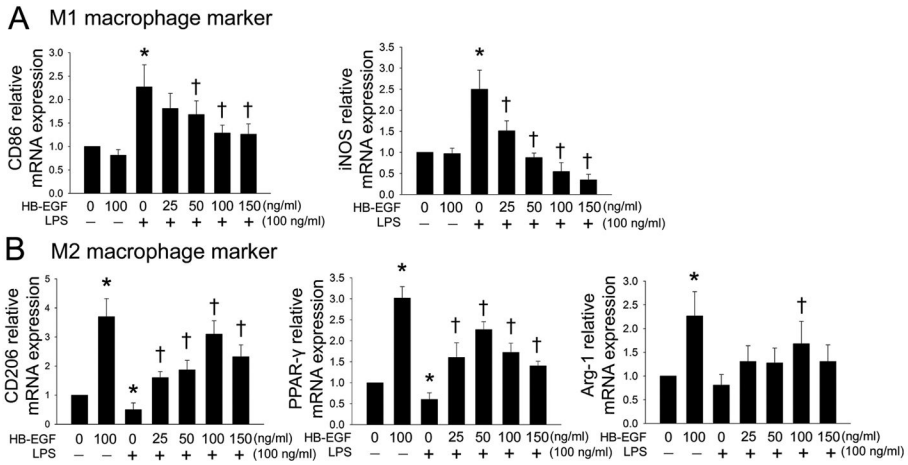

Figure 4. Effect of HB-EGF on M2 macrophage polarization as determined by quantitative real time PCR

Macrophages derived from THP-1 cells were exposed to the indicated conditions × 24h and then harvested for mRNA extraction. mRNA expression of the indicated genes was examined using qRT-PCR. The transcript level of each gene was normalized against the level of unstimulated macrophages, which was arbitrarily set as 1. Data represent the mean ± SD of three independent experiments, with each experiment performed in triplicate. (A) M1 macrophage associated markers. * $p<0.05$ *vs.* **control;** † $p<0.05$ *vs.* LPS alone. (B) M2 macrophage associated markers. * $p<0.05$ *vs.* con**trol;** † $p<0.05$ *vs.* LPS alone.

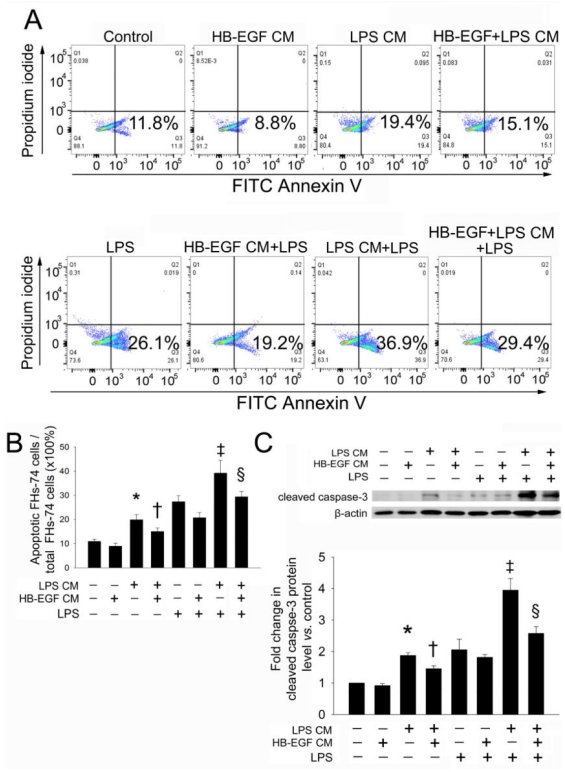

Figure 5. Effect of HB-EGF treatment of macrophages on LPS-induced FHs-74 cell apoptosis

(A) Macrophages derived from THP-1 cells were either unstimulated or exposed to HB-EGF (100ng/ml), LPS (100 ng/ml), or HB-EGF (100 ng/ml) + LPS (100 ng/ml) for 24h. Cells were then washed in PBS and fresh medium added. Supernatant were collected 8h later as Control CM, HB-EGF CM, LPS CM or HB-EGF + LPS CM. FHs-74 cells were cultured in CM alone or in CM + LPS (1 μg/ml) for 24h, and then harvested for Annexin V/PI flow cytometry. Gating was performed on FITC-Annexin V^+ cells. (B) Quantification of results of A, Data represent the mean ± SD of four independent experiments. Statistical analysis was performed with ANOVA followed by Bonferroni's multiple comparison test. * $p<0.05$ *vs.* no addition **control; † $p<0.05$** vs. **LPS CM alone; ‡** $p<0.05$ *vs.* LPS alone; § $p<0.05$ *vs.* LPS CM+LPS. (C) Western blot analysis of cleaved caspase-3 expression in FHs-74 cells. The expression level of cleaved caspase-3 was normalized against the level of FHs-74 cells incubated with control CM, which was arbitrarily set as 1. Data represent the mean ± SD of three independent experiments. * $p<0.05$ *vs.* **control; † $p<0.05$ vs. LPS CM alone; ‡** $p<0.05$ *vs.* LPS alone; § $p<0.05$ *vs.* LPS CM+LPS.

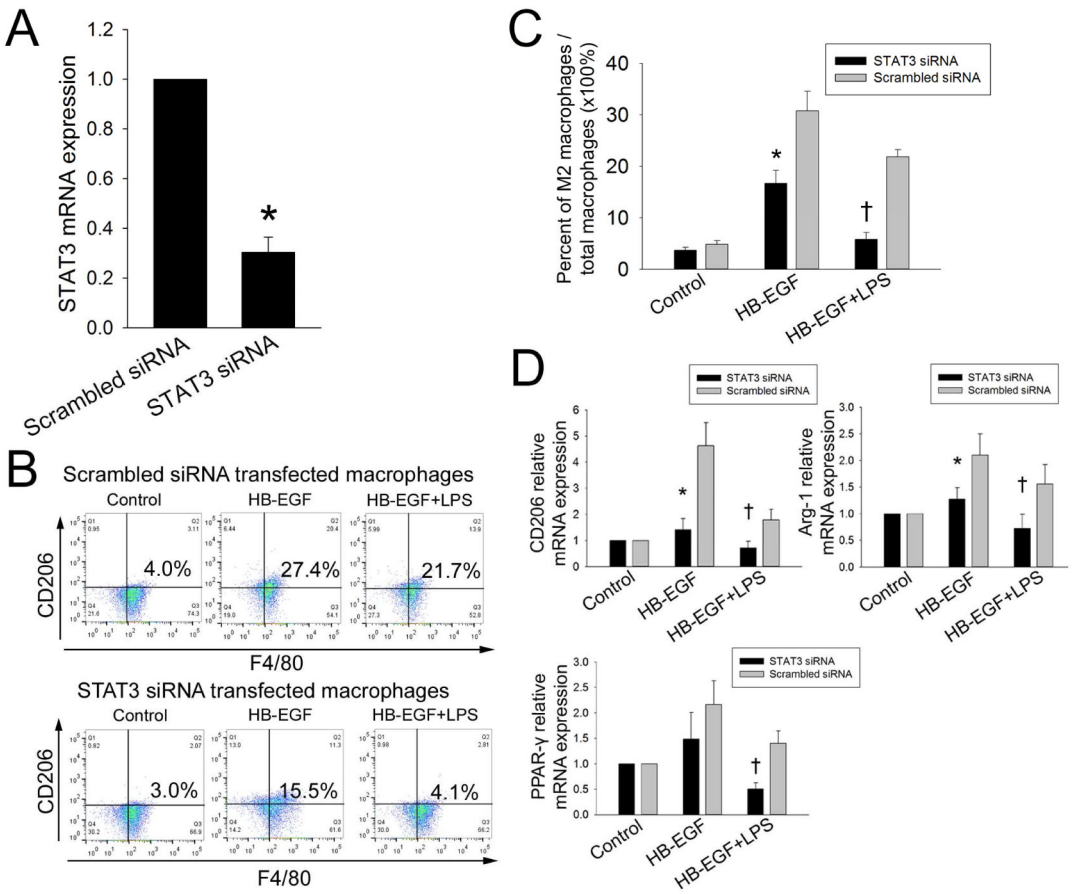

Figure 6. Effect of HB-EGF on STAT3 activation during HB-EGF macrophage polarization

(A) Silencing efficiency of STAT3 siRNA in macrophages as determined by real-time PCR. **p*<0.05 *vs.* scrambled siRNA. (B) Macrophages derived from THP-1 cells were transfected with either scrambled control siRNA or STAT3 siRNA and were then exposed to the indicated treatments for 24h. M2 macrophages were labeled with PE-Cy5-conjugated anti-human CD206 and APC-conjugated anti-human F4/80 antibodies and then analyzed the percentage of M2 macrophages/total macrophages by flow cytometry. Representative FACS plots are shown. Gating was performed on $CD206^{+}/F4/80^{+}$ cells. (C) Quantification of data from B. * *p*<0.05 *vs.* scramble siRNA transfected MØ+HB-EGF**;** † *p*<0.05 *vs.* scramble siRNA transfected MØ+HB-EGF+LPS. (D) mRNA expression of M2 associated markers was examined using real time PCR. The transcript level of each gene was normalized against the level of unstimulated macrophages, which was arbitrarily set as 1. Data represent the mean ± SD of four independent experiments.

* *p*<0.05 *vs.* scramble siRNA transfected MØ+HB-EGF**;** † *p*<0.05 *vs.* scramble siRNA transfected MØ+HB-EGF+LPS.

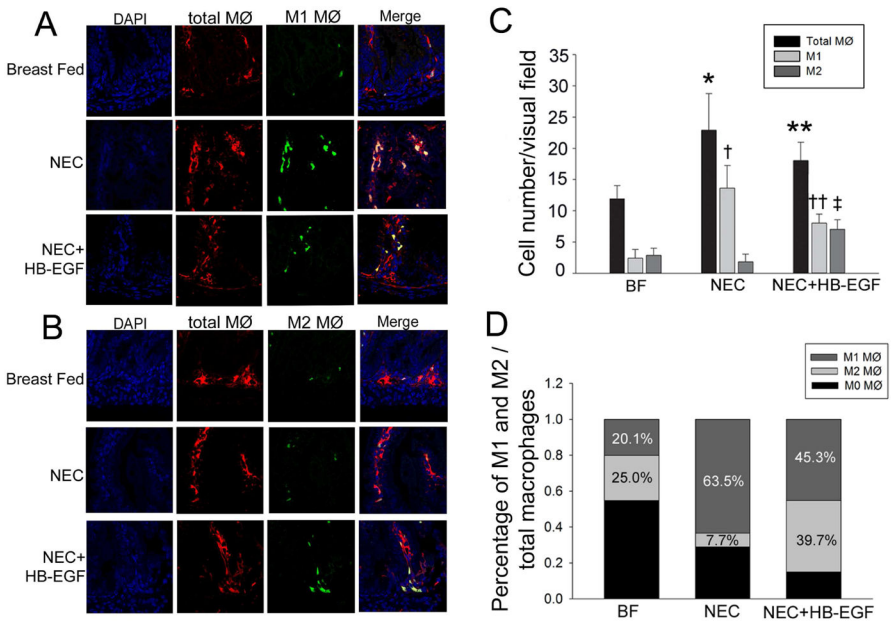

Figure 7. Effect of HB-EGF on macrophage infiltration and polarization during NEC

(A) Representative immunofluorescent staining for the total macrophage marker CD68 (red) and the M1 macrophage marker CD86 (green) of intestinal sections obtained from mouse pups exposed to breast feeding (n=12), NEC (n=12), or NEC + HB-EGF (n=12). Nuclei are indicated by DAPI staining. M1 macrophages are indicated by co-localization of CD68 and CD86 in the merged images. (B) Representative immunofluorescent staining for the total macrophage marker CD68 (red) and the M2 macrophage marker CD206 (green). Nuclei are indicated by DAPI staining. M2 macrophages are indicated by co-localization of CD68 and CD206 in the merged images. In A and B, eight segments of intestine were analyzed for each mouse pup, and four fields in each section were viewed and counted blindly by two independent investigators. (C) Quantification of the results from A and B. Data represent mean ± SD. * $p<0.01$ *vs.* BF; **<0.05 *vs.* **NEC; †**$p<0.05$ *vs.* **BF; ††$p<0.05$ vs. NEC; ‡** $p<0.05$ *vs.* NEC. (D) Quantification of the percent of macrophage subtypes in intestinal sections from mouse pups exposed to the indicated treatments. Data represent mean ± SD. Statistical analysis was performed with ANOVA followed by Bonferroni's multiple comparison test.

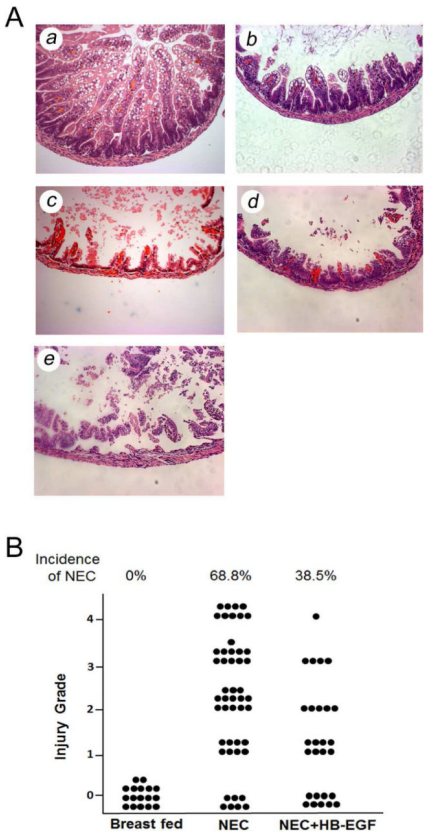

Figure 8. Effect of HB-EGF on the incidence and severity of NEC

Intestinal samples were harvested from breast fed mouse pups (n=17), pups exposed to NEC (n=48), or pups exposed to NEC and treated with HB-EGF (n=27), and sections stained with H&E. (A) Representative examples of histological scoring of intestines. Eight to ten segments of intestines were analyzed for each mouse pup. Each section were viewed and graded blindly by two independent investigators. Magnification ×20. (*a*) Grade 0, normal intestine; (*b*) Grade 1, epithelial cell lifting or separation; (*c*) Grade 2, necrosis to mid villus level; (*d*) Grade 3, necrosis of entire villus; (*e*) Grade 4, transmural necrosis. Any injury of grade 2 or above is considered consistent with NEC. (B) Incidence and severity of NEC. Each dot represents an individual mouse pup.

Table 1

a

Gene	NCBI ref. sequence	Primer
M1 Macrophages		
iNOS	NM_001002837	SENS: GTTCTCAAGGCACAGGTCTC REVS: GCAGGTCACTTATGTCACTTATC
CD86	NM_175862	SENS: TGGAGAGGGAAGAGAGTGAACA REVS: GCCCATAAGTGTGCTCTGAA
M2 Macrophages		
CD206	NM_002438	SENS: CCATGGACAATGCGCGAGCG REVS: CACCTGTGGCCCAAGACACGT
Arg-1	NM_001244438	SENS: TTCTCAAAAGGACAGCCTCG REVS: GCTCTTCATTGGCTTTCCC
PPAR-γ	NM_138712	SENS: TCCTGTAAAAGCCCGGAGTAT REVS: GCTCTGGTAGGGGCAGTGA

*a*Table 1. Primers for RT-PCR.